THE ASTROPHYSICAL JOURNAL, 430:121–138, 1994 July 20

MORPHOLOGICAL STUDIES OF THE GALAXY POPULATIONS IN DISTANT "BUTCHER-OEMLER" CLUSTERS WITH *HST*. I. AC 114 AT $z = 0.31$ AND ABELL 370 AT $z = 0.37$[1]

WARRICK J. COUCH
School of Physics, University of New South Wales, P.O. Box 1, Kensington NSW 2033, Australia
AND
RICHARD S. ELLIS, RAY M. SHARPLES, AND IAN SMAIL
Department of Physics, University of Durham, South Road, Durham, DH1 3LE, UK
Received 1993 October 25; accepted 1994 January 21

ABSTRACT

We present the first results of an ongoing program we are undertaking with the Wide Field Camera of the *Hubble Space Telescope* (*HST*) to understand the physical origin of the enhanced star formation seen in moderate-redshift ($z \sim 0.3$–0.4) cluster galaxies. Deep *HST* exposures have been obtained for the central regions of two rich compact "Butcher-Oemler" clusters, AC 114 at $z = 0.31$ and Abell 370 at $z = 0.37$. Both of these clusters have been subject to extensive ground-based spectroscopic and multiband imaging studies with a significant fraction of *confirmed* members being seen in the active or ensuing phases of a starburst. We have used the *HST* images in conjunction with the ground-based data to examine the morphology of individual cluster members, in particular these "starburst" objects. We find that those blue members that display spectral evidence of active or recently completed star formation are predominantly disk-dominated systems whose abundance is greater than that seen in the cores of present-day rich clusters. Furthermore, ~55% of the galaxies in this category in both clusters show convincing evidence of dynamical interactions, in contrast to a 20%–30% rate of occurrence among the red population. While similar conclusions had been drawn from high-quality ground-based data, we demonstrate the unique role *HST* can play in identifying interacting galaxy pairs which have separations less than the current resolution limits of the best ground-based images. There is convincing evidence in these first two clusters we have examined that interactions and mergers play a major role in inciting the star formation activity associated with the Butcher-Oemler effect.

Of equal significance is the morphological nature of the numerous *red* members in our *HST* data set which show various spectroscopic and photometric indications of previous starburst activity, including strong Balmer-line absorption. Most of these galaxies appear to be undisturbed and isolated with a normal E morphology. There is no convincing evidence that these are merger products.

Although larger samples are still required, we conjecture that the Butcher-Oemler effect may involve at least two physical processes arising from the hierarchical growth of clusters: galaxy-galaxy interactions and environmentally induced star formation arising from the hierarchical merging of clusters. Much work remains to be done to understand exactly how the fraction of disk galaxies seen in distant rich clusters declines to its present low value.

Subject headings: galaxies: clusters (AC 114, Abell 370) — galaxies: interactions — galaxies: photometry — galaxies: stellar content

1. INTRODUCTION

A major focus in observational cosmology over the last decade or more has been the mounting evidence for galaxies in the rich cluster environment having undergone significant evolution over the last one-third of a Hubble time. The first to present evidence for such evolution were Butcher & Oemler (1978) whose photometry of two rich concentrated clusters at $z \sim 0.4$ indicated an excess population of blue galaxies in comparison to that seen in present-day clusters. This result—now commonly known as the "Butcher-Oemler" (BO) effect—motivated numerous observational programs which have targeted high-redshift clusters for further broadband photometry (Butcher & Oemler 1984; Couch & Newell 1984), detailed multiband optical and infrared imaging work (Couch et al. 1983; Ellis et al. 1985; MacLaren, Ellis, & Couch 1988; Aragón-Salamanca, Ellis, & Sharples 1991), and spectroscopic investigations (Dressler & Gunn 1982, 1983; Lavery & Henry 1986; Couch & Sharples 1987, hereafter CS). These studies established that the BO effect is both widespread in rich clusters at $z \geq 0.2$ and can be ascribed to a subset of the cluster members either undergoing or having recently completed a vigorous short-lived burst of star formation.

The identification of the BO effect as a starburst-related phenomenon raises the question as to the series of events which triggered such activity at these earlier epochs and yet led to its demise by the present day. The quest for a single mechanism that can explain the diverse observational features discussed above has received much attention (see Oemler 1992 for an excellent review). At the most fundamental level, the observation that local galaxies of a given morphological type show environmental differences in their star formation characteristics and abundances could indicate the transformation of

[1] Based on observations with the NASA/ESA *Hubble Space Telescope*, obtained at the Space Telescope Science Institute, which is operated by the Association of Universities for Research in Astronomy, Inc., under NASA contract NAS 5-26555.

properties with time ("nurture") or a change in the relative formation rates ("nature"). However, even at modest redshifts, differences in the observed galaxy proportions may primarily reflect luminosity changes, particularly if abrupt star formation events are involved. Allington-Smith et al. (1993) claim the rising blue fraction witnessed by Butcher & Oemler is *not* seen in less rich groups identified via radio galaxies—an environment intermediate between rich clusters and the field—and propose the BO effect is largely a rich-cluster phenomenon which, in turn, may explain the origin of the local density-morphology relation.

What physical processes might have occurred in rich clusters as recently as 3–4 Gyr ago, yet be absent in their present-day counterparts? Dressler & Gunn (1982, 1983) proposed the perturbing action of a shock front in the hot intracluster gas on the interstellar medium of infalling gas-rich field galaxies. On entering the cluster, their star formation would initially increase but then be truncated as the gas was swept away. Such an explanation attributes star formation to external sources, so the question of evolution in the long-standing member galaxies is not addressed. Evrard (1991) modeled such ram pressure effects in some detail and found qualitative agreement with the observations. However, in a more recent analysis of published spectroscopic and photometric data in 14 distant clusters, Allington-Smith et al. claimed to find little convincing evidence for dynamical or spatial segregation between the red and blue members, in contrast to Evrard's predictions.

An alternative viewpoint is that the evolution is largely in genuine cluster members from their interaction with one another and/or the intracluster medium. Ram pressure stripping was proposed by Gunn & Gott (1972) as a possible mechanism for producing the highly abundant S0 population seen in local clusters. Further support is provided by the redder colors of spirals in clusters compared to their counterparts in the field (Butcher & Oemler 1984). However, as Oemler (1992) points out, the absence of a strong correlation between spiral fraction and X-ray luminosity is worrying if stripping is an important factor. Mergers and interactions between galaxies are promising and can lead to S0s if the gas is driven into the hybrid nucleus, or to an elliptical if the disk is disrupted. Additionally, tidal encounters can lead to bursts of star formation without morphological changes. Lavery and coworkers (Lavery & Henry 1988; Lavery, Pierce, & McClure 1992, hereafter LPM) have presented evidence for galaxy interactions and mergers being the primary cause, based on high-resolution CCD imagery of the distant blue populations conducted from the ground.

The importance of securing morphological data for representative star-forming galaxies in distant clusters has long been recognized as the most valuable observational method to make progress in understanding this long-standing puzzle in observational cosmology. In an attempt to discriminate between the various explanations discussed above, we have commenced a program to utilize the excellent spatial resolution of the *HST* to morphologically classify the galaxy populations in distant BO clusters. Our efforts concentrate on those clusters we have studied previously either spectroscopically (CS) or through multiband optical and infrared imaging (MacLaren et al. 1988; see also Aragón-Salamanca et al. 1991).

The spectroscopic study undertaken by CS with the multi-object fiber (FOCAP) system on the 3.9 m Anglo-Australian Telescope (AAT), generated 4 Å resolution spectra of $\sim$150 objects within the fields of three rich clusters at $z = 0.31$. Importantly, these high-quality data allowed the star formation activity of cluster members to be assessed individually using the combination of Balmer "Hδ" index and broadband color. This approach revealed significant samples of blue and red galaxies in either the ongoing or subsequent phases of starburst activity. The multiband photometric studies concentrated primarily on the early-type galaxies. By examining the spectral energy distributions across a wide wavelength range, examples were found of optically red galaxies with excess light at ultraviolet and near-infrared wavelengths. We will refer to these as the "UVX" and "IRX" sources, respectively. In the case of the UVX sources, MacLaren et al. (1988) attributed the light at a rest-frame wavelength of $\sim$270 nm to a small residual main-sequence population from recent star formation. For the IRX sources, Aragón-Salamanca et al. (1991) proposed the excess K-band light arises from the late stages of stellar evolution also associated with recent star formation. These papers attempted to interpret such signatures in terms of a single cycle of star formation activity seen at various stages, a hypothesis that can be directly tested with morphological information.

In this paper we present the first results of our study, based on deep exposures with the *HST* Wide Field Camera (WFC), of the rich centrally concentrated clusters AC 114 at $z = 0.31$ and Abell 370 at $z = 0.37$. AC 114 was the most comprehensively studied cluster within the CS spectroscopic sample. In contrast, Abell 370 has detailed multicolor information from which UVX and IRX populations were identified. Spectroscopic data on this cluster are also available through the studies of Henry & Lavery (1987; hereafter HL) and Soucail et al. (1988; hereafter SMFC), providing us with some scope to classify members following the precepts adopted by CS for AC 114. High-resolution (FWHM $\sim$0.″5) ground-based imagery of Abell 370 has been conducted by LPM using the HRCAM system on the 3.6 m Canada-France-Hawaii Telescope (CFHT). Their images of the blue members reveal a high ($\sim$50%) incidence of multiple systems with many claimed to be undergoing interactions/mergers. Our *HST* image of Abell 370 provides an independent check on these results and, in doing so, an instructive comparison between *HST* imagery and that taken in the best seeing conditions currently achieved from the ground.

The organization of this paper is as follows: in § 2 we describe our *HST* observations and the steps taken in processing the data. In § 3 we address the spectroscopic classification of the imaged galaxies, including new and deeper spectroscopy for AC 114. Our morphological classification procedure for the distant cluster galaxies is described in § 4. A comparison of our classifications with those of LPM together with an examination of the connection between morphology and star formation activity is also presented in this section. Our results are discussed and summarized in § 5.

2. HST IMAGING

The WFC observations of AC 114 and Abell 370 were obtained during the periods 1991 November 19–25 and 1992 November 10, respectively. AC 114 was observed as part of a GO cycle 1 allocation originally awarded to image all three of the CS clusters but which we subsequently devoted to a single cluster following the discovery of spherical aberration in *HST*'s primary mirror. The observations of Abell 370 were made in Director's discretionary time awarded to a parallel distant cluster imaging program conducted by A. Dressler,

TABLE 1

LOG OF *HST* OBSERVATIONS

Cluster	R.A.(2000)	Decl.(2000)	Date	Filter	P.A.(V3)	Exposure (s)
AC 114	$22^h58^m47^s.01$	$-34°48'13''.5$	1991 Nov 19–20	F555W	242.464	15300
			1991 Nov 22	F555W	243.800	6900
			1991 Nov 23	F814W	243.800	6900
			1991 Nov 24–25	F814W	244.689	13800
Abell 370	02 37 21.87	−01 47 15.5	1992 Nov 10	F702W	196.230	17600

A. Oemler, H. Butcher, and J. Gunn,[2] who kindly made their data available to us. A log of the observations is given in Table 1; included are the J2000 coordinates at which our images were centered, the dates, the filters used, the telescope position angles (V3 axis), and the total exposure times. The exposures are mostly composed of a series of 2300 s integrations taken during successive orbits of the telescope. The filters employed, F555W, F702W, and F814W, closely match the standard Johnson *V*, *R*, and *I* bands. respectively.

The AC 114 data were received from the Space Telescope Science Institute in the form of individual frames with the standard pipeline procedures of bias removal and flat-field division applied. We found the latter to be unsatisfactory due to the inadequate flat-field exposures used, especially in the F814W filter. A complete rereduction of all the frames was therefore performed at the Space Telescope European Coordinating Facility (ST-ECF), Garching, using new and much improved flat fields. The frames were then combined using a 3 σ cosmic-ray rejection algorithm to give final coadded frames for each position angle. Most of the frames in each filter were taken at a single orientation. Although we have resampled and coadded the data taken at different orientations, given the importance of maintaining the maximum possible spatial resolution in the final images, we chose to base most of the analysis in this paper on the coadditions of the primary orientations which represent exposure times of 13,800 s and 15,300 s in F555W and F814W, respectively. Our median coaddition algorithm removed all the cosmic-ray events and a substantial fraction of the "hot spots"—low-level single-pixel features present on all four of the WFC CCDs which do not flat-field out. The remaining hot spots were eliminated using the method developed by Adorf (1993). For Abell 370, the data were supplied to us as final coadded images (both restored and unrestored; see below) having already been subjected to a similar series of processing steps by Dressler and described in detail in Dressler et al. (1993). Fortunately, these data were all taken at a single position angle.

While some imperfections still remained in the data at this stage—CCD blemishes, residual large-scale gradients in the background, and faint ghost images—the frames were nonetheless striking in the high-definition images they provided of the cluster galaxies (see Fig. 1). One immediately noticeable example is an $R = 19.5$ member of AC 114 (*top-center*, in Fig. 1), which is resolved very clearly as a face-on late-type spiral galaxy. Also very conspicuous are the gravitational "arcs" in these fields, none more so than the one in Abell 370 originally recognized by Soucail et al. (1987). The use of our WFC data to study gravitational lensing effects in these and other clusters will be the subject of a separate paper (Smail et al. 1994, in preparation). In the context of the present study, it is clear that our 4–5 hr exposures have ensured that the $18 < R < 21$ cluster galaxies have a sufficient signal-to-noise ratio (S/N) in the much diminished core of the aberrated *HST* point-spread function (psf) to fully realize the high ($\sim 0''.1$) resolution information that it contains. The only encumbrance is that all the objects are surrounded by large halos, a fact we account for in the morphological classification process (see § 4).

The aberrated psf of *HST* has led to much debate on the merits of image deconvolution (Adorf 1993; Elson & Schade 1993). Given that a high S/N in the *HST* psf core has been obtained for our cluster galaxies, we can thus expect only a marginal improvement in this image quality when the exposures are deconvolved. To illustrate this, Figure 2 shows three examples of F555W images in AC 114 before and after deconvolution. The frames were first sync-interpolated onto a finer grid before being deconvolved using subsampled psf's created using the TINYTIM package (Krist 1992). To accomplish the restoration we used 40 iterations of the accelerated Lucy-Richardson algorithm implemented by Richard Hook at

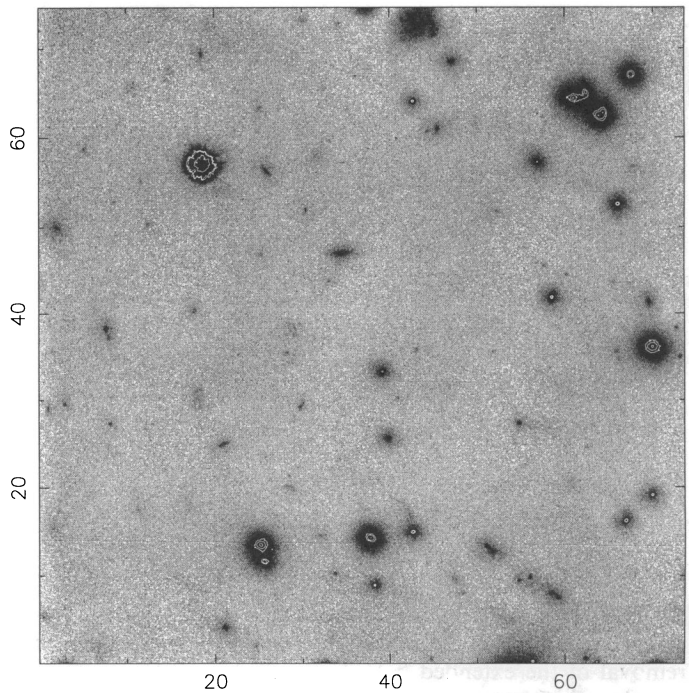

FIG. 1.—Northeastern quadrant of the final coadded but unrestored image of AC 114 taken with the *HST* WFC through the F555W filter. The graduated scale around the perimeter of the image indicates arcseconds; the vertical direction (*bottom to top*) is oriented at a position angle of 27°.5.

[2] The first results of which are reported in Dressler et al. (1994, hereafter DOGB); see also Dressler et al. (1993).

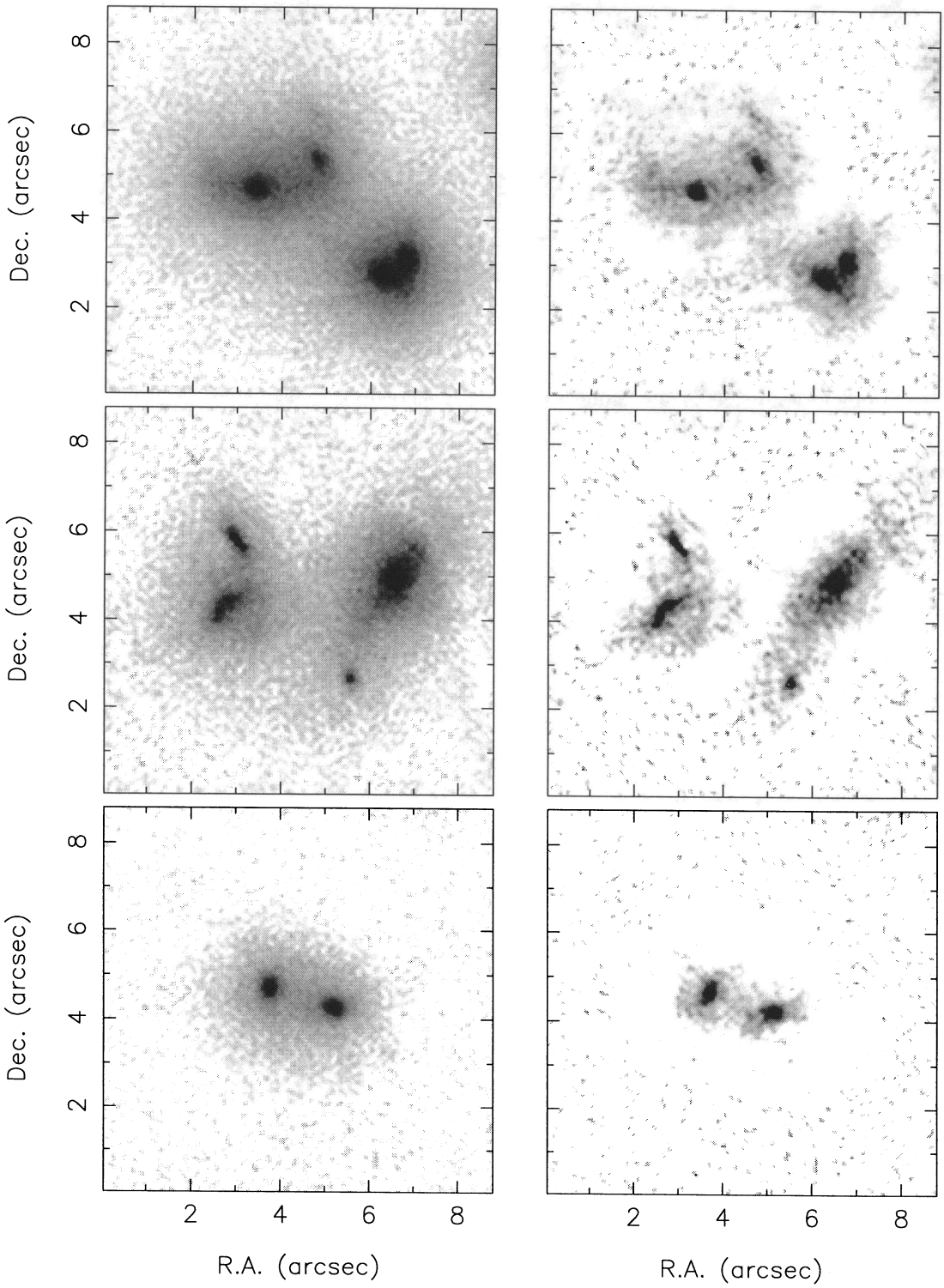

FIG. 2.—Three examples of F555W images of AC 114 cluster members prior to (*left*) and after (*right*) deconvolution.

ST-ECF. It is apparent that there are only small gains in the resolution of some structures, the main change being the removal of the extended halos around objects. However, we feel that this improvement is more than offset by the large amount of spurious low-level structure introduced into the images and the sharpening of residual artifacts. As our investigation is exploratory at this stage and does not involve matching surface brightness profiles to data for images known a priori to obey representative (e.g., $r^{1/4}$) laws, our analysis is based on *unrestored* versions of our final coadded frames.

3. SPECTROSCOPIC DATA

The thrust of our *HST* program is to study spectroscopically confirmed cluster members, particularly those whose star for-

mation characteristics are understood in terms of the indicators discussed in § 1. Here we assemble the available information for AC 114 and Abell 370, including new spectroscopic results for AC 114.

3.1. *New Spectroscopy of AC 114*

A cursory inspection of our WFC images of AC 114 quickly convinced us that they contain valuable morphological information for galaxies fainter than the magnitude limit of the original CS sample ($R = 20$). Accordingly, we returned to the AAT to extend the original spectroscopic sample to deeper limits using the Low Dispersion Survey Spectrograph (LDSS-1). The primary aim was to obtain spectroscopy in the WFC field in the range $20 < R \leq 21$, the depth to which we consider that morphological detail can be discerned. A secondary aim was to obtain spectra for the seven galaxies in the WFC field at $R \leq 20$ not observed by CS. This provided a list of 34 targets, 24 of which were accommodated in three multislit aperture masks manufactured for our program. All eight of the blue ($B-R \leq 2$) objects in our initial list were purposely included in this total of 24. Four objects previously observed by CS outside the WFC field were also included on each mask to provide a cross-check on our measurements.

Our LDSS-1 observations were carried out on the nights of 1992 September 20 and 21. The "high-dispersion" grism was used, yielding a dispersion of 164 Å mm^{-1} which, with slits of width 1".5, resulted in a spectral resolution of ~ 10 Å. A thinned 1024 × 1024 24 μm pixel Tektronix CCD was used as the detector, providing a wavelength coverage of 4000 Å $< \lambda <$ 8000 Å. The weather on the two nights was mixed, allowing total integrations in clear conditions of 12,600 s and 6410 s for each of two masks. The seeing varied from 1".5 to 2".0 (FWHM).

The data were reduced using a combination of routines in the LEXT (Colless et al. 1990) and FIGARO spectral reduction packages. After bias subtraction, the five to six individual integrations on each mask were stacked and cleaned of cosmic-ray events using the LDSS-STACK routine kindly supplied by K. Glazebrook. The rectangular region enclosing the dispersed light from each slit was then extracted from the stacked frame and wavelength-calibrated using the two-dimensional calibration derived from the same region of the arc exposure for that mask. A weighted sky subtraction was then performed using an interactive procedure to manually select the spatial bounds of the object and bracketing sky regions to ensure an accurate interpolation of the sky underneath the object.

A representative selection of the reduced spectra are shown in Figure 3 where the familiar spectroscopic signatures found by CS can be seen. In terms of quality, the new spectra are comparable to those obtained by CS; their S/Ns range from 3 to 15 (with a median of 6), thus providing spectral line measurements of precision greater than or equal to that achieved by CS. Such measurements of the median observed wavelength and equivalent width (EW) of the identifiable emission and absorption lines were conducted using the FIGARO routine ABLINE. Redshifts were derived by taking the mean of the values calculated for the measured features in each spectrum.

A synopsis of these measurements plus other relevant data is given in Table 2. For each of the objects observed we list their identification number (Couch & Newell 1984), R.A. and Decl. (1950), R-magnitude, $B-R$ color, redshift, and, where applicable, the equivalent widths measured for the [O II] λ3727 emission and Hδ absorption lines. The uncertainties in the Hδ equivalent width values, quoted because of the importance of Hδ as a spectral type indicator (see below), are taken from the [S/N, ϵ(EW)]–relation derived empirically by CS from model synthetic spectra.

As can be seen, the LDSS-1 observations have yielded spectra for an additional 15 objects in the AC 114 field, 13 of which are cluster members and two of which are background objects. The last four objects listed in Table 2 are the repeated CS objects; a comparison of their redshifts with those derived by CS indicates agreement at the $\Delta z = \pm 0.0019$ level. Similarly, we find the equivalent widths agree to within their uncertainties.

Combining our new data with the earlier CS measurements yields a total of 31 spectroscopically confirmed members within our WFC field. The composition of this sample in terms of spectroscopic type can be seen in Figure 4 where the [EW(Hδ), $(B-R)_{obs}$]–diagram is plotted (the distribution of the objects in the color-magnitude plane is also shown as an

TABLE 2

LDSS-1 SPECTROSCOPY OF AC 114

CN	R.A.(1950)	Decl.(1950)	R	$B-R$	z	EW(λ3727) (Å)	EW(HHδ) (Å)	Spectral Type
30	$22^h56^m03^s.99$	−35°03′43″.6	21.13	2.49	0.3169			E/S0:
40	22 55 59.66	−35 04 14.7	19.96	2.36	0.3123		2.6±0.9	HDS
53	22 56 05.96	−35 04 27.0	20.80	2.48	0.3157			E/S0
90	22 56 03.19	−35 03 15.0	21.19	2.49	0.3326			E/S0:
105	22 55 58.92	−35 03 32.2	20.01	2.35	0.3185			E/S0
111	22 56 00.25	−35 03 36.3	19.87	1.40	0.3131	55.3	−1.1±1.0	Starburst
112	22 56 00.00	−35 03 37.1	20.47	2.34	0.3157			E/S0
115	22 55 57.49	−35 03 55.8	20.96	1.47	0.326			E/S0:
119	22 55 55.94	−35 03 45.8	20.52	2.44	0.3107			E/S0
121	22 55 55.58	−35 03 26.7	20.38	1.77	0.503	68.8		Starburst:
139	22 55 58.89	−35 04 21.4	20.58	2.55	0.3264			E/S0
143	22 55 56.47	−35 04 36.2	20.47	1.67	0.3122		10.1±1.0	PSG
146	22 55 56.78	−35 04 53.1	20.19	1.42	0.3047	11.1	8.3±0.7	PSG
161	22 55 59.33	−35 05 08.7	20.84	1.74	0.5703	34.8		Spiral:
188	22 56 02.81	−35 05 07.9	20.53	2.32	0.3190			E/S0
438	22 55 54.33	−35 06 19.8	19.85	1.21	0.3156	31.0	5.9±0.7	
616	22 56 09.42	−35 01 41.4	19.21	2.20	0.3323	6.6	3.4±0.8	
797	22 55 51.37	−35 05 30.1	19.38	2.47	0.3177		3.6±0.7	
832	22 55 48.37	−35 03 09.2	19.98	2.25	0.3204		4.8±0.9	

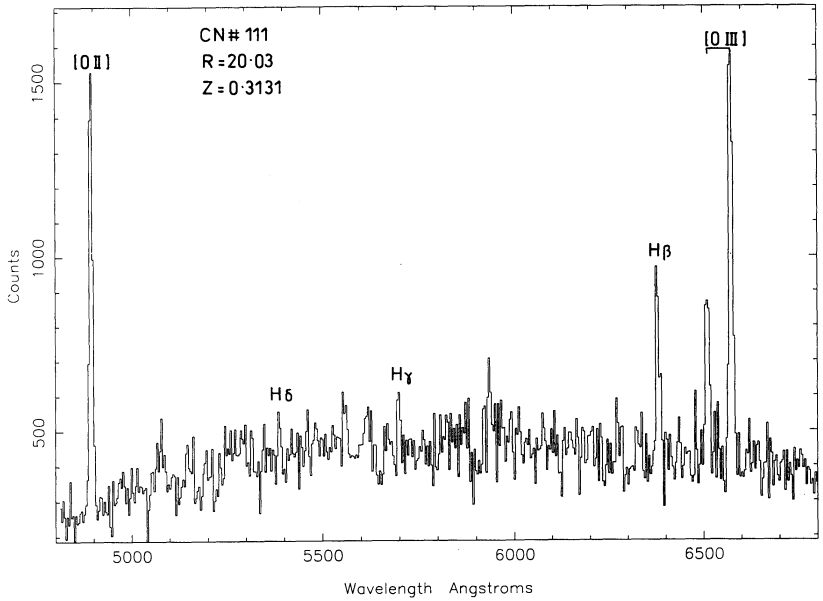

FIG. 3*a*

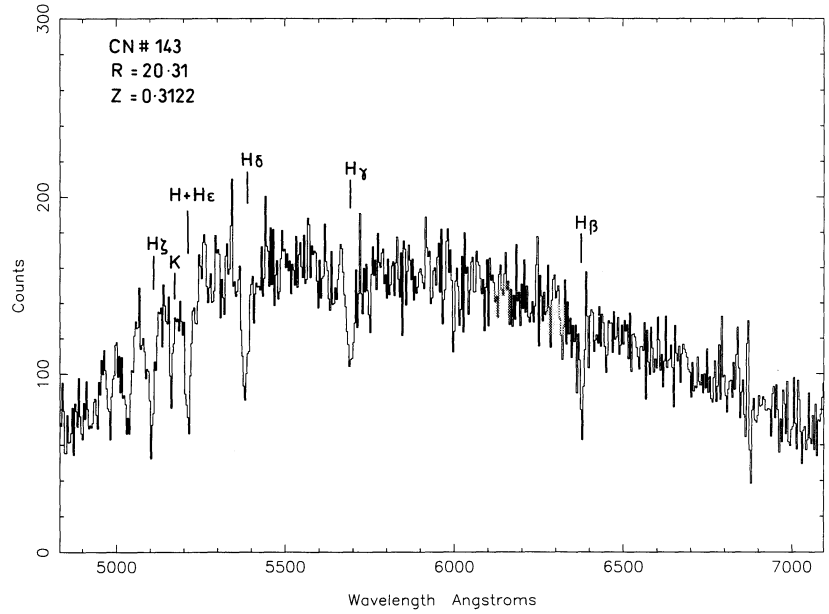

FIG. 3*b*

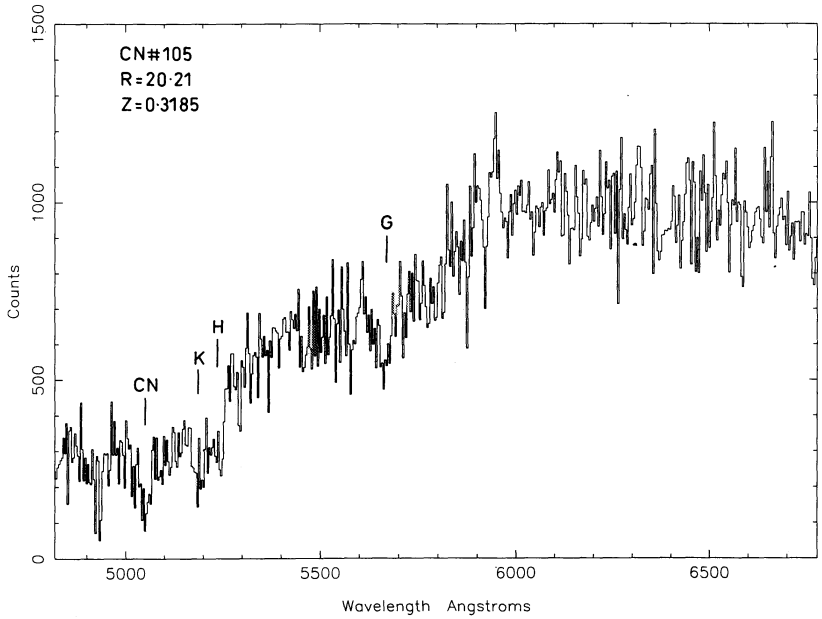

FIG. 3*c*

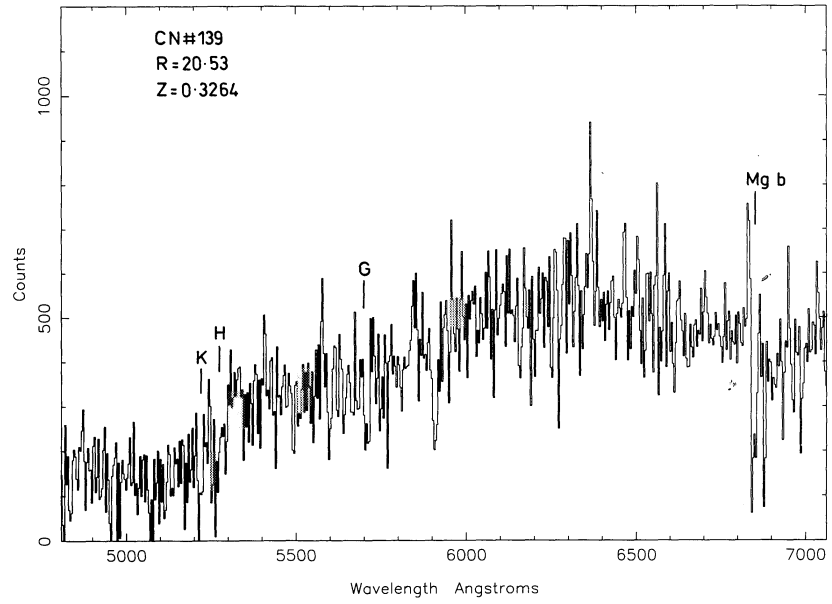

FIG. 3*d*

FIG. 3.—Representative LDSS-1 spectra obtained of AC 114 cluster members. *Abscissa*: observed wavelength; *ordinate*: CCD counts. Prominent absorption and emission line features are identified.

inset). As CS demonstrated, the distant cluster galaxies occupy quite distinct regions of this diagram dependent upon their star formation activity. Objects undergoing a burst of star formation (labeled "starburst" in Fig. 4) are characterized by blue colors and emission-filled Hδ lines and thus reside in the bottom left-hand corner of the diagram. The "post-starburst" (PSG) types are similarly blue but have moderate to strong (EW > 4 Å) Hδ absorption. Galaxies with the spectral characteristics of nearby spirals lie along a sequence of increasing Hδ strength with bluer color as indicated by the cross-hatched region in Figure 4. Within the red galaxy population, CS found a dichotomy in Hδ strength. Those objects with little or no Hδ absorption (EW ≤ 2 Å) resemble the nearby E/S0 galaxy population in terms of their spectra and rest-frame colors. The red galaxies with prominent (EW > 2 Å) Hδ, on the other hand, are interpreted as the products of starbursts occurring in previously dormant galaxies and seen 1–2 Gyr following the completion of the burst. We shall hereafter refer to these latter types as "HDS" galaxies.

Using this spectroscopic classification, for AC 114 we have 11 "active" objects in total (those labeled in Fig. 4), consisting of two starburst galaxies (87 and 111), three PSG galaxies (22, 143, and 146; the latter also shows weak [O II] λ3727 emission, indicating some residual ongoing star formation), one spiral galaxy (74), and five HDS galaxies (4, 40, 89, 187, and 858). The remaining 20 members are in the "inactive" E/S0 class. Spectral classifications for the new objects in the LDSS-1 sample are given in the last column of Table 2. Note that the three red members whose spectral type is denoted by "E/S0:" are cases where the S/N, and hence the precision of the Hδ measurement, is too low to confidently exclude the possibility that they are HDS objects [EW(Hδ) > 2 Å]; as such, they have not been included in Figure 4. The complete set of confirmed members within our WFC field, grouped according to spectral type, is listed in Table 3.

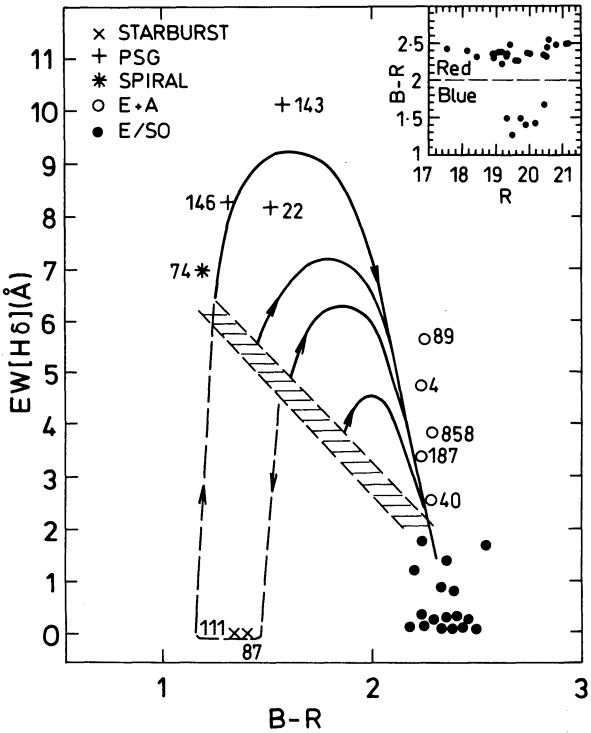

FIG. 4.—Hδ equivalent width vs. $(B-R)_{obs}$ diagram of Couch & Sharples (1987). The points in the diagram represent the spectroscopically confirmed members of AC 114 which lie within our WFC field; their spectroscopic classifications, based on their position in the diagram, are indicated in the legend. The arrowed dashed-solid and solid lines represent evolutionary tracks from the starburst and truncated star formation models, respectively, of Couch & Sharples (1987; see their paper for details). The cross-hatched area represents the region of the diagram occupied by present-day spiral galaxies. *Inset*: distribution of the same AC 114 members in the $[(B-R), R]_{obs}$ color-magnitude plane.

3.2. *Collation of Data for Abell 370*

Spectroscopy for ~90 objects within an ~6′ × 6′ field centered on Abell 370 is available from HL and SMFC. HL's multislit spectroscopy conducted on the CFHT yielded spectra with a resolution of 16 Å and a wavelength coverage of 5100–7000 Å for ~30 blue and red galaxies with $N \leq 20.4$. They have published the redshifts measured from their spectra and, for the 18 objects confirmed as members, measurements of EW(Ca II H + Hε)/EW(Ca II K) and continuum slope, F_ν(5000 Å)/F_ν(4100 Å). Plots of the spectra for nine of the members are also presented. The observations of SMFC, carried out at the CFHT and on the ESO 3.6 m telescope, provide spectra for 84 objects with a resolution of 10–20 Å and a wavelength coverage of either 4500–7200 Å or 4500–6700 Å. The faintest object in their catalog has $N = 20.6$. SMFC present plots of all their spectra together with redshifts and a spectral type based on a comparison with synthetic spectra from Guiderdoni & Rocca-Volmerange (1987). There are 18 galaxies common to both the HL and SMFC studies.

Unfortunately, the S/N of these spectra is often poor, and it is thus not possible to carry out a spectral typing of galaxies according to the quantitative approach of CS. Instead we have classified galaxies qualitatively from the available spectral plots using as a reference representative spectra from CS. To do this we examined each spectrum for the distinctive absorption/emission line features and continuum shape, taking into account the spectral typings given by MacLaren et al. (1988) and SMFC. The results of this procedure for all the Abell 370 members within our WFC field are presented along with other relevant information in Table 4. To aid in the cross-referencing of objects, their numbers under the identity schemes used by Couch & Newell (1984; as also MacLaren et al. 1988), SMFC, and Butcher, Oemler, & Wells (1983) are given in the first three columns, respectively.

Following the practice of CS, we have distinguished galaxies as being either "red" or "blue" and the data in Table 4 are listed accordingly. The basis for this distinction is the distribution of objects within the color-magnitude plane, constructed using the $N, J-N$ photographic photometry of Butcher et al. (presented here in cols. [5] and [6] of Table 4) and shown as Figure 5. This figure reveals a clear division of the data into a "red" E/S0 color-magnitude sequence and a population of "blue" objects below it. Formally, we take a value of $J-N = 2.3$ as the dividing line between the two populations.

Although the spectral data for Abell 370 are of lesser quality, there is more complete ground-based photometry. Specifically, from the studies of MacLaren et al. (1988) and Aragón-Salamanca et al. (1991), we can examine those red galaxies with photometric excesses (UVX and IRX) that may indicate recent star formation. The red galaxies are therefore subgrouped to distinguish these particular types (as well as the spectroscopically identified HDS galaxies) from the ordinary E/S0 class. Although some of the UVX and IRX galaxies were not

TABLE 3

AC 114 WFC SAMPLE

CN (1)	R (2)	$B-R$ (3)	Interaction/Merger (4)	Morphology (5)	Comments (6)
			E/S0		
1.....	17.54	2.42	Dist	cD	
3.....	18.15	2.39		E	
6.....	18.90	2.34		E	
26.....	18.93	2.35	Int(2″.0)	B	
2.....	18.94	2.35		I	
159.....	18.94	2.28		S0	
145.....	19.18	2.37		B	
5.....	19.19	2.20	Sat(2″.7)	I	
232.....	19.35	2.35		I	
8.....	19.42	2.48		S0	
176.....	19.68	2.24		B	
105.....	20.01	2.35	Int(1″.5)	E	
112.....	20.47	2.34	Sat(2″.7)	E	Satellite of No. 5
119.....	20.52	2.44		I	
188.....	20.53	2.32		S0	
139.....	20.58	2.55	Dist	E	
53.....	20.80	2.48		B	
115.....	20.96	1.47		B	
30.....	21.13	2.49		B	
90.....	21.19	2.49	Dist	B	
			HDS		
4.....	18.44	2.31		E	Round
858.....	19.12	2.37		E	Round
187.....	19.31	2.31	Dist	I	
89.....	19.61	2.25		E	Round
40.....	19.96	2.36		E	
			Starburst		
87.....	19.32	1.48	Int(1″.5)	I	
111.....	19.87	1.40	Merg(0″.3) + Int(1″.6)	D	
			Post-starburst		
22.....	19.73	1.49	Merg(0″.5)	D	
146.....	20.19	1.42		B	
143.....	20.47	1.67		I	
			Spiral		
74.....	19.47	1.27		Sc–Sd	Face-on spiral

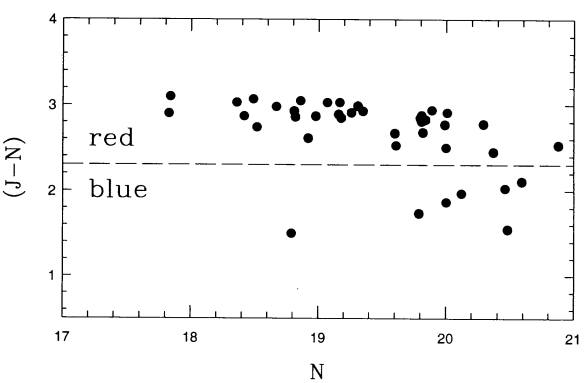

FIG. 5.—Color-magnitude diagram for the spectroscopically confirmed members of Abell 370 in our WFC sample. *Abscissa*: N-magnitude; *ordinate*: $(J-N)$ color. The photometry is from Butcher, Oemler, & Wells (1983).

observed spectroscopically by HL or SMFC, MacLaren et al.'s spectral energy distributions constructed from multiband CCD photometry are consistent with their being cluster members. Note that a number of galaxies are listed as having a spectral type "E/S0:"; as in § 3.1, this indicates cases where the spectrum had the general characteristics of an E/S0 galaxy but had an S/N too poor to have any hope of recognizing it as an HDS object on the basis of the strength of its Balmer lines. Those cases where the spectral type was undetermined are, in all categories, denoted by a question mark.

The lists in Tables 3 and 4 represent near-magnitude-limited samples that lie within the WFC field ($R < 21$–21.2 for AC 114 and $N < 20.6$–20.9 for Abell 370). A comparison between Couch & Newell's (1984) R-band photometry of Abell 370 and that published in the N-band by Butcher et al. indicates an average offset for cluster members of $R-N \sim 0.2$ mag. Thus the samples extend down to approximately the same apparent magnitude limit in each cluster but accordingly probe to slightly different luminosities by virtue of the different redshifts. The two samples are also somewhat complementary. In AC 114, we

TABLE 4

ABELL 370 WFC SAMPLE

CN (1)	SMFC (2)	BO (3)	z (4)	N (5)	J-N (6)	Spectral Type (7)	UVX (8)	IRX (9)	Interaction/Merger (10)	Morphology (11)	Comments (12)
						Red					
107.....	35	9	0.374	17.83	2.90	E/S0				cD	
125.....	23	21	0.3695	18.36	3.03	E/S0				E	
42.....	9	24	0.377	18.42	2.87	E/S0:			Int(1.″8)	E	
31.....	17	26	0.382	18.49	3.07	E/S0			Sat(1.″4)	E	
47.....	13	34	0.378	18.67	2.98	E/S0:				E	
32.....	54	43	0.3825	18.82	2.86	E/S0:				E	
49.....	16	45	0.369	18.86	3.05	E/S0				I	Boxy bulge
101.....	37	49	0.369	18.92	2.61	E/S0			Int(0.″8)	I	Associated galaxy Merg (0.″32)
36.....	74	55	0.363	18.98	2.87	E/S0			Sat(1.″1)	E	
15.....	52	61	0.383	19.07	3.03	E/S0				S0	
68.....	8	66	0.3695	19.18	2.85	E/S0:			Dist	B	
83.....	53	70	0.377	19.26	2.91	E/S0:				E	
164.....	45	75	0.38	19.31	2.99	E/S0:			Int(1.″2)	B	
12.....	87	80	0.386	19.35	2.93	E/S0				S0	
62.....	4	107	0.37	19.61	2.53	?				I	
23.....	29	133	0.37	19.81	2.88	?				E	
100.....	83	136	0.375	19.82	2.68	E/S0:			Sat(1.″8)	E	
58.....	68	163	0.3685	19.99	2.77	E/S0			Sat(2.″8)	B	
18.....	64	166	0.3625	20.00	2.50	E/S0?				B	
116.....	81	167	0.384	20.01	2.91	E/S0:				S0	
87.....	86	311	0.362	20.88	2.53	E/S0:				E	
29.....	18	41	0.376	18.81	2.93	HDS		X	Dist?	E/S0	
79.....	11	149	0.382	19.89	2.94	HDS			Dist, Merg?	D	Two-component system?
81.....	32	...	0.370	18.44[a]	2.00[a]	E/S0:	X	X	Int(4.″2)	E	
20.....	28	29	0.3715	18.52	2.74	E/S0	X	X		E	
86.....	36	106	0.372	19.80	2.85	E/S0	X	X	Sat(2.″6)	E	
46.....	12	...	0.375	19.69[b]	1.17[b]	E/S0?	X		Dist	D	Lies on arclet
69.....	7	131	0.378	19.81	2.81	E/S0	X			B	
109.....	91	142	0.371	19.84	2.83	?	X		Sat(1.″3)	I	
1.....	20	10	0.3785	17.84	3.10	E/S0		X		cD	
94.....	56	...	0.382	19.09[a]	2.95[a]	E/S0		X		E	Compact nucleus
80.....	31	62	0.368	19.16	2.89	E/S0		X		E	
22.....	27	63	0.3885	19.17	3.03	E/S0		X		S0	
105.....	63	...	0.370	19.48[a]	2.86[a]	E/S0		X	Int(3.″6)	E	
4.....	76	...	0.373	20.00[a]	2.77[a]	E/S0:		X		B	
27.....	30	105	~0.37	19.60	2.67	?	X			E	
84.....	...	203	~0.37	20.29	2.78	...	X			S0	
11.....	...	219	~0.37	20.37	2.45	...	X			B:	Falls on CCD join
103.....	...	...	~0.37	20.46[c]	2.30[c]	...	X			B	
102.....	...	...	~0.37	20.53[c]	2.14[c]	...	X			I	
						Blue					
66.....	10	39	0.375	18.79	1.50	PSG			Merg	?	Merger remnant, three tidal tails
70.....	70	128	0.36	19.79	1.74	PSG			Sat(2.″2)	D	
90.....	34	165	0.387	20.00	1.87	Spiral			Dist	D	
99.....	...	181	0.390	20.12	1.97	?				E	
85.....	...	239	0.384	20.48	1.55	Spiral?			Merg?	D(pec)	Disturbed system
77.....	...	236	0.367	20.46	2.03	...			Sat(0.″9, 1.″2)	D	Triple system
45.....	71	256	0.37	20.59	2.11	PSG					B

[a] R and $B-R$ values of SMFC.

[b] R and $B-R$ values of SMFC, but the latter claimed by LPM to be erroneously blue.

[c] R_F and $B_J - R_F$ values of Couch & Newell 1984.

are able to spectroscopically categorize individual galaxies, whereas in Abell 370, the precision is largely in the photometric definition, particularly of red members.

4. MORPHOLOGICAL CLASSIFICATION OF CLUSTER MEMBERS

An initial inspection of the ~70 confirmed members on our WFC images of AC 114 and Abell 370 indicates a variety of morphologies including systems structurally similar to nearby elliptical, lenticular, and spiral systems, disturbed galaxies, and a noticeable number of interacting systems. These impressions served to focus the quantitative classification of cluster galaxies on the following two issues:

1. *Involvement in an interaction and/or merger with another galaxy.*—A key question given the evidence presented by Lavery and coworkers.

2. *Description in terms of a nearby analogue.*—Can the distant cluster galaxies be placed within the present-day Hubble sequence?

This scheme was applied independently by three of us

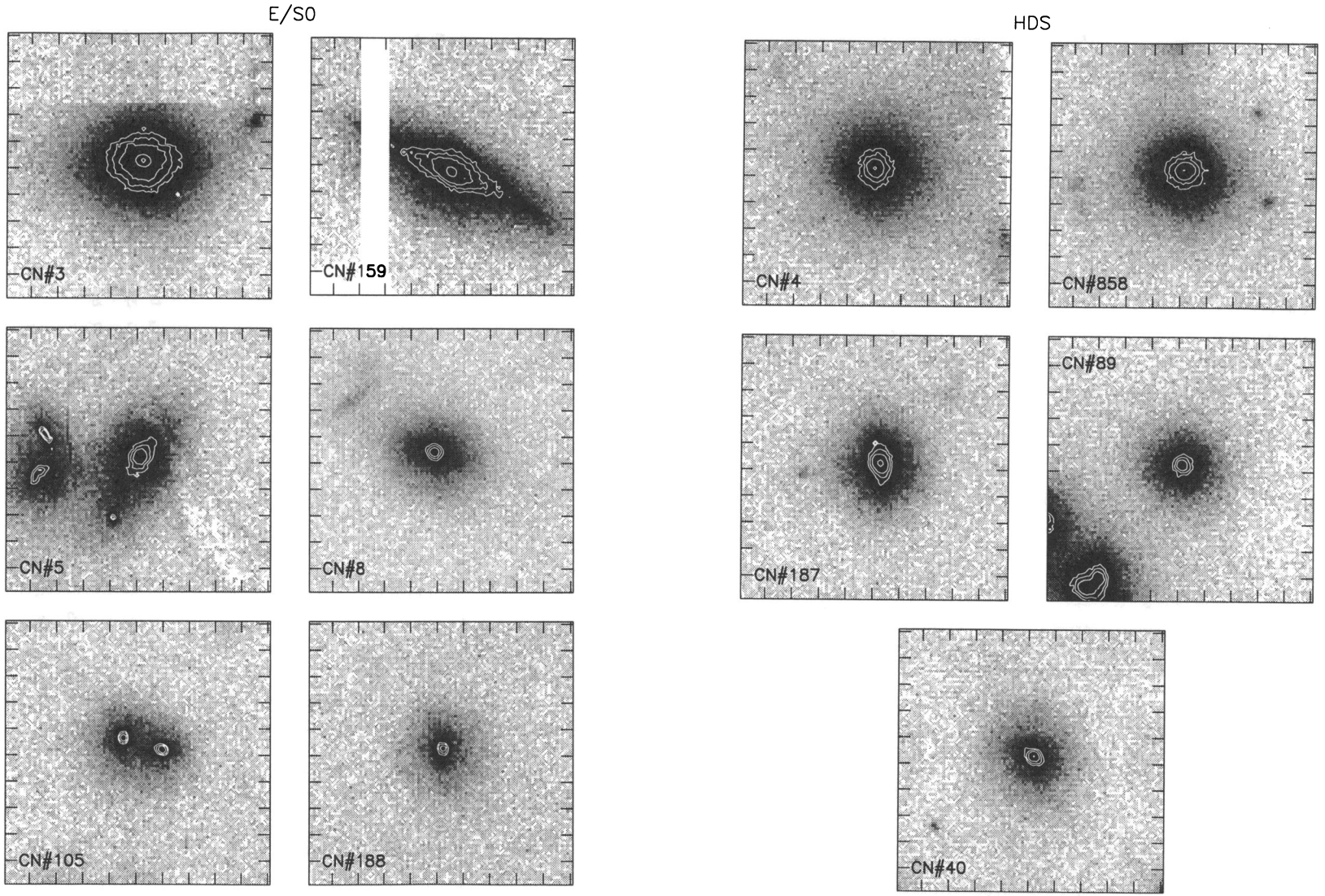

FIG. 6.—WFC images of individual members of AC 114 taken from the final coadded (but unrestored) F555W frame of the cluster. Objects are grouped according to their spectroscopic classification (see text for details). Arcsecond graduations are marked around the perimeter of each image.

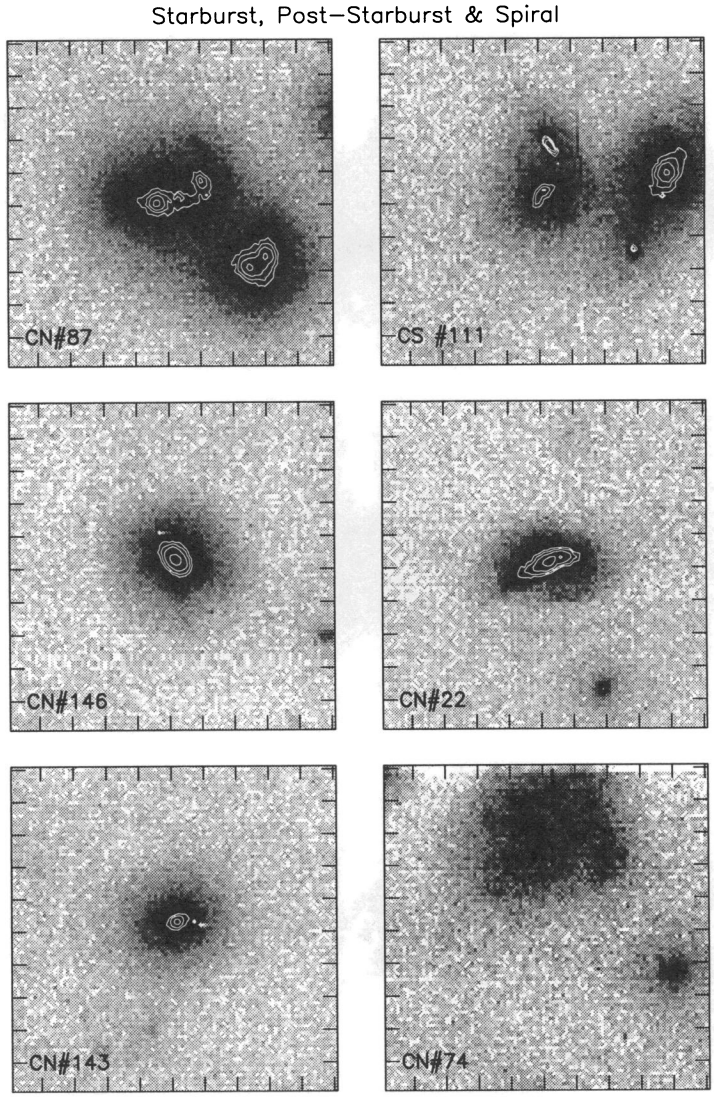

FIG. 6.—*Continued*

(W. J. C., R. M. S., and I. S.) to the spectroscopic samples listed in Tables 3 and 4. This resulted in a consensus on classifications for ~75% of the galaxies; in the remaining cases there was always agreement between two of us and so the majority view was adopted. Before presenting these results, we first describe our approach to issues 1 and 2 above in more detail and discuss the additional morphological information provided by the two-color imagery of AC 114. We then compare our classifications individually with those of LPM, which serves to illustrate the advantages and disadvantages of *HST* data in comparison to high-quality ground-based images on larger aperture telescopes. Finally we turn to the critical question of a possible connection between the morphologies deduced and the various indicators of star formation identified earlier.

To substantiate our classifications, Figures 6 and 7 present the WFC images of selected individual members. In Figure 6, the images for the AC 114 members are grouped according to the spectroscopic types (starburst, PSG, HDS, E/S0) discussed in § 3.1, and in Figure 7, the members of Abell 370 are grouped according to their photometric class (red, blue, UVX, IRX).

4.1. *The Identification of Interactions and Mergers*

While the presence of a nearby companion may draw attention to objects possibly undergoing a tidal interaction or merger, their significance is difficult to evaluate because the local surface density is a strong function of position within the cluster. A major advantage of our *HST* data over ground-based observations is that, at $z \simeq 0.35$, the 0".1 resolution corresponds to physical scales of $\sim 0.5\ h^{-1}$ kpc where connected isophotes, isophotal distortions, and/or tidal tails can be directly identified.

Within this framework, we can identify three generic situations:

1. Systems where a double structure is discerned just above the resolution limit of the data (i.e., separations ~0".2–0".5, $\sim 1.0\ h^{-1}$ kpc, at $z = 0.35$); these are galaxies most likely in an advanced stage of merging—examples include Nos. 22 and 111 in AC 114 (Fig. 6).
2. Systems with spatially distinct but tidally linked components of comparable brightness such as No. 87 in AC 114 and CN 101 in Abell 370.

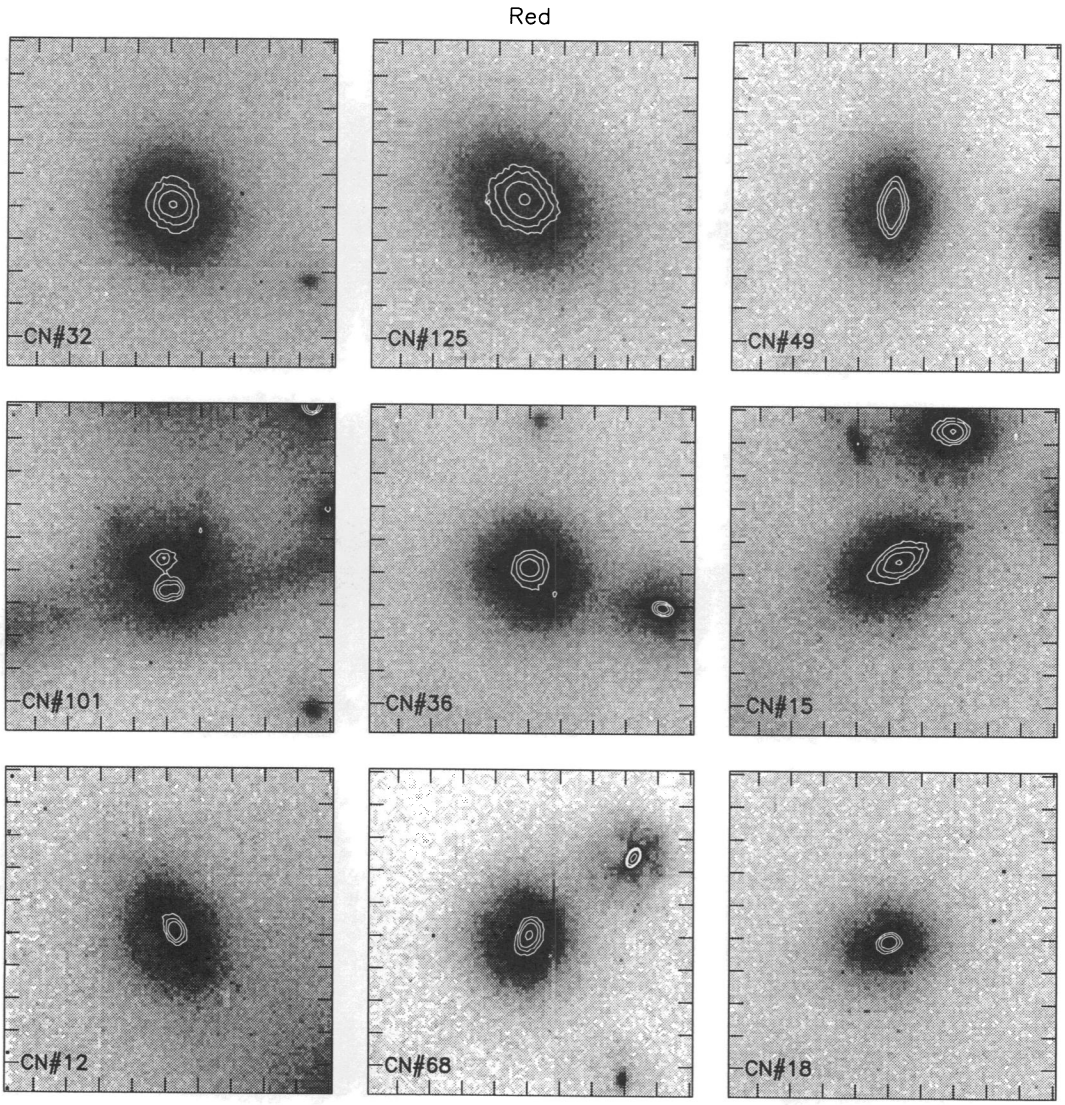

FIG. 7.—As for Fig. 6 for Abell 370. The images come from the final coadded (but unrestored) F702W frame; members are grouped according to their photometric classification (see text for details).

3. Systems where the associated galaxy is a much fainter "satellite" such as CN 70 in Abell 370 and No. 5 in AC 114.

We were also vigilant for isolated objects which bear the hallmarks of a recent tidal/merger event as evidenced by tidal tails, prominences, and/or a disturbed appearance (Toomre & Toomre 1972). Two cases were found in Abell 370—CN 66 and CN 79. No examples were found among the confirmed members in the AC 114 field but a red galaxy, No. 25, within Couch & Newell's (1984) photometric sample has a curved tail 5″ in extent emanating in a northeasterly direction.

A total of 23 galaxies within AC 114 and Abell 370 were identified in this way as candidate interactions/mergers. These objects are indicated as such in column (4) of Table 3 and column (8) of Table 4 with cases 1, 2, and 3 above being distinguished by the abbreviations "Merg," "Int," and "Sat," respectively. The separation in arcseconds between the components of these systems follows in parentheses. In addition, a number of galaxies have been listed as "Dist," indicating systems with distorted outer isophotes.

4.2. *Individual Galaxy Morphologies*

The morphological classification of the cluster samples (irrespective of any involvement in an interaction or merger) was done on a galaxy-by-galaxy basis in two stages. First we identified those galaxies which could be unambiguously assigned a Hubble type (E, S0, Sa–Sd). A total of 40 galaxies were classified in this way, most being the brightest ($R \leq 20$) red galaxies, typed spectroscopically as E/S0 or HDS and which in all cases were classified morphologically as cD, E, or S0. Only one spiral was found—the blue galaxy No. 74 in AC 114 which is a face-on Sc–Sd.

As a benchmark for this exercise we used a ground-based CCD image of the core of the Coma cluster convolved with a TINYTIM model psf to simulate a view of a nearby rich cluster at a *physical* resolution ($\sim 0.5\, h^{-1}$ kpc) and S/N similar to those realized by our WFC imagery of AC 114 and Abell 370 at $z \sim 0.35$. This was particularly useful in estimating the accuracy with which E and S0 types could be separated, using morphological classifications from Dressler (1980b) as a refer-

Red–HDS & Red–UVX

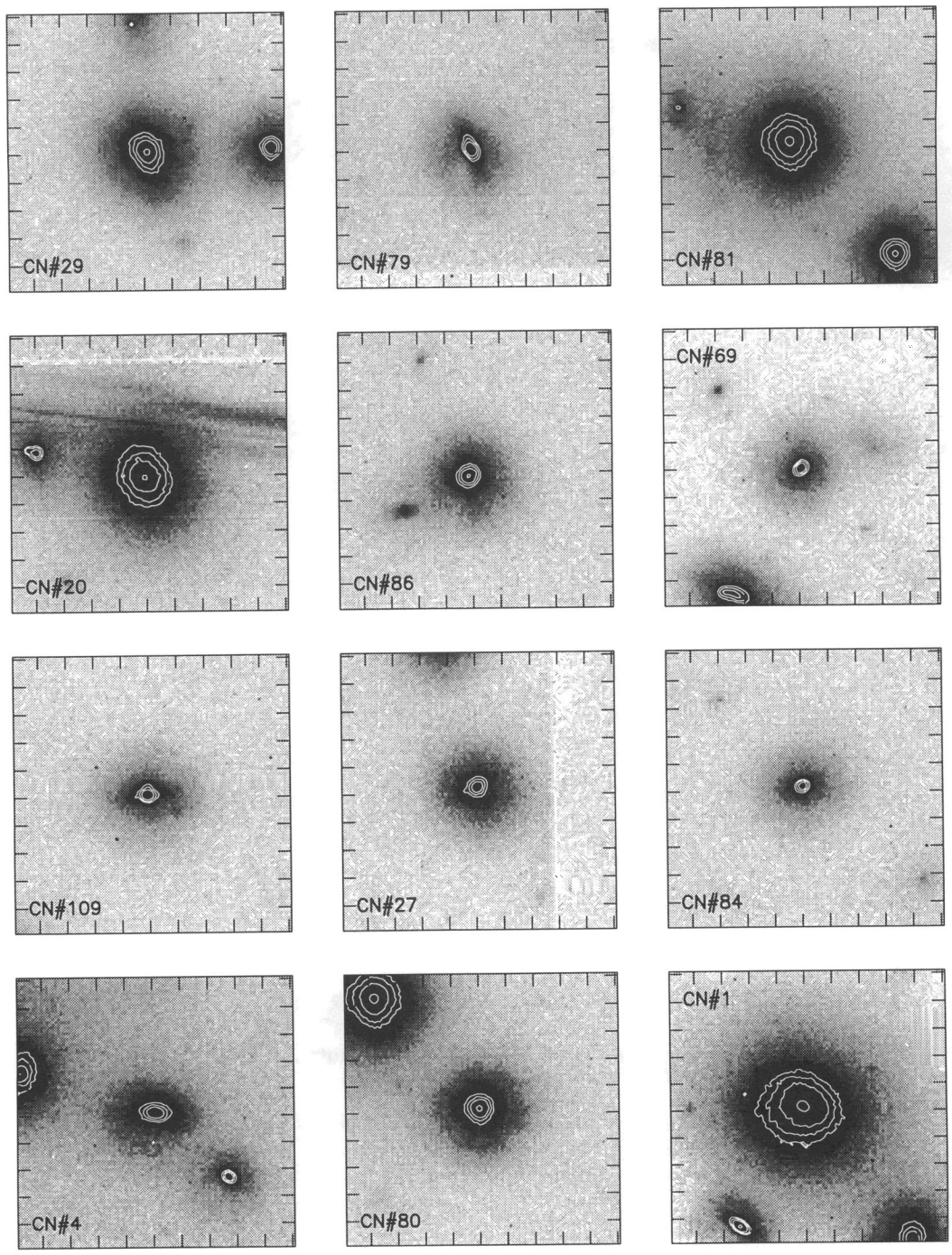

FIG. 7.—*Continued*

ence. Within the area of our CCD frame, Dressler classified six E and 13 S0 galaxies (excluding borderline cases) down to the approximate absolute luminosity limit reached by the *HST* frames in the distant clusters. Blind classification of these galaxies on the raw CCD image resulted in "correct" identifications for 92% of the Es and 85% for the S0s (borderline cases were given half-weight). After the CCD image was convolved with the *HST* psf and degraded to the appropriate S/N, however, only 15% of the Es were correctly identified and 31% of the S0s were mistyped as Es. This experiment confirmed the difficulty of differentiating between E and S0 galaxies on our *HST* images unless the latter are highly inclined. Less than one-third of S0s would be expected to have ellipticities less than E7 on the basis of random inclinations, although in prac-

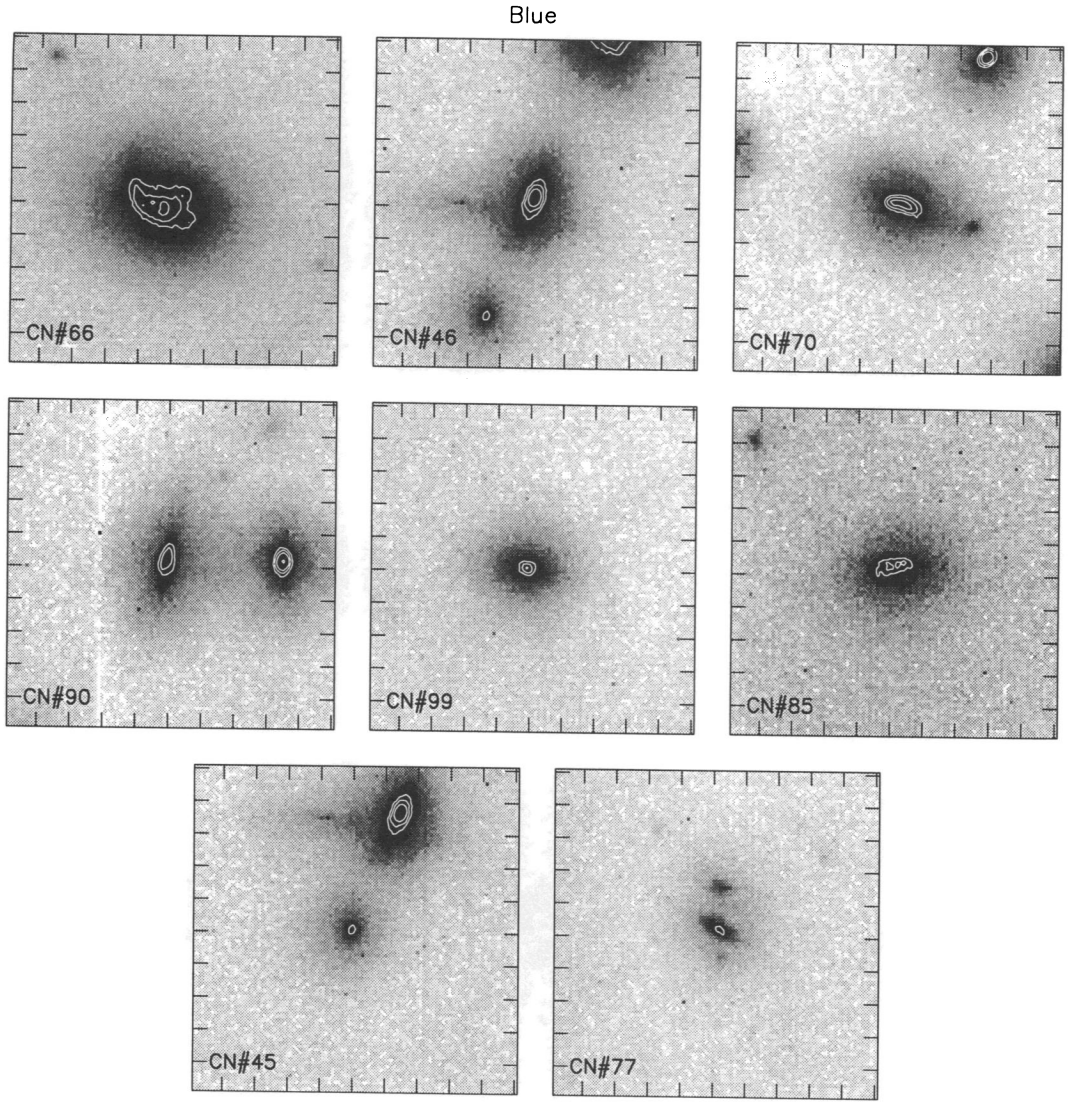

FIG. 7.—*Continued*

tice the distinctive disk features of S0s are recognizable at lower inclinations, even in data with limited resolution, provided that the S/N is adequate.

The galaxies not classified in this first stage were generally systems too faint or small for us to confidently judge their Hubble class. Nonetheless, bulge and/or disk components could always be seen in these galaxies. Dressler (1980a), in his morphological studies of nearby galaxy populations, stressed the importance of the bulge-to-disk ratio, B/D, as a discriminator of galaxies in different environments. We have therefore based the morphological classification of the remaining cluster members on the relative dominance of the bulge or disk components, labeling them either as bulge-dominated (B), disk-dominated (D), or of intermediate morphology (I). The correlation Dressler found between B/D and Hubble type would indicate that these three classes correspond to approximate groupings of the E/S0, Sc–Sd, and Sa–Sb types, respectively.

A listing of our morphological classifications can be found in column (5) of Table 3 and column (11) of Table 4 with the B, D, I bulge-disk notation used for objects not assigned a specific Hubble class.

4.3. *The Two-Color Imagery of AC 114*

In the context of describing our procedural approach to morphologically classifying the distant cluster galaxies, the additional information yielded by having both V (F555W) and I (F814W) imagery of AC 114 requires further comment. Although these bands correspond roughly to rest bands B and R, there were *no* significant differences in the morphologies observed for our galaxy sample between the different colors. While the structural details of galaxies were slightly more accentuated in V than I, this did not amount to differences in the assigned interaction/merger class or individual morphologies (as detailed in §§ 4.1 and 4.2) between the two colors.

The two-color data available for AC 114 also enabled us to examine specific object classes in two colors. Two-dimensional $(V-I)$ color maps were created in order to examine possible spatial color variations. For most objects no extra morphological information was revealed. In the specific case of systems

where there is ongoing star formation or those in the PSG phase, this would suggest that the light from their young stellar population is, to first order, distributed uniformly over the galaxy.

One interesting result did emerge for the HDS galaxies in AC 114. Because the resampling necessary to align the two frames in this procedure could create spurious effects (due to the undersampling of the peak of the psf), we compared the HDS results with those for a similarly distributed sample of "normal" E galaxies. Of the five HDS objects in the WFC field, four resemble the normal Es with no spatial color gradient outside the central 0".1–0".2 of the galaxy. However, one HDS galaxy (CN 89) shows structural differences between the two passbands on scales which are incompatible with resampling errors. This object contains a roughly V-shaped blue region, 1" in extent, whose apex is centered on the galaxy core. This structure is on the west side of the galaxy and may indicate a disruption event deep in the galaxy core.

4.4. *Comparisons with the Ground-based Imagery of Lavery et al. 1992*

A total of eight cluster members within our Abell 370 WFC field were also imaged in the high-resolution study of LPM. These happen to be the entire subset of "blue" galaxies grouped in Table 4 plus the red UVX galaxy CN 46 (≡SMFC 12). Table 5 compares the interaction/merger and morphology information that each group has derived for these eight galaxies.

For BO 128, BO 181, and BO 236 both studies agree closely. For the remaining objects there are differences that merit discussion and we now do this individually:

BO 39.—This galaxy is claimed by LPM to be an interacting system consisting of a "tail and large low surface brightness extension" separated by 0".9. We classified this galaxy as a merger remnant on the basis of its disturbed appearance plus tidal prominences but no resolvable double structure. While we are unclear on precisely how LPM define a multiple-component system, this object is probably a case where the higher resolution of our WFC images has been critical in discerning its true structure. Indeed, our data show it to be much more complex, with a bright irregular core with a long curved tail in one direction and two fainter and shorter inwardly curved tails in the opposite direction.

SMFC 12.—Our higher resolution data are able to settle the uncertainty LPM discussed as to whether the associated orthogonal faint feature is a tidal tail or a gravitational "arclet." Figure 7 shows this feature exhibits the same thin lacelike appearance of other known arcs in the cluster and is not characteristic of any other tidal tails. We conclude that this feature is the gravitational lensed image of a background object and has no association with this cluster member.

BO 165.—LPM claim this to be interacting with a satellite object 3" to its northwest. While this companion is visible on our WFC image, there is no discernible connection of isophotes between the two. However, the connection is seen in LPM's image by virtue of their deeper limiting surface brightness.

BO 239.—While this galaxy is isolated, LPM made no reference to its peculiar structure. The *HST* image reveals a curious L-shaped appearance consisting of a dominant disk with a protuberance at one end. There is also a hint of a short and very faint curved tidal feature originating from the opposite end. We believe this is suggestive evidence for a merger product.

BO 256.—LPM mention a possible tidal tail associated with this object (just distinguished in their published image), which is not seen in the *HST* image.

While comparisons have been possible for only a small number of objects, the exercise has nonetheless given some general indications of the relative merits of the space-based and ground-based high-resolution imagery of distant galaxies. Clearly the 0".4–0".5 resolution LPM achieved is sufficient to reliably identify the gross morphological features of galaxies and, in most cases, their involvement in interactions/mergers. The *HST* data demonstrate that the extra level of detail realized at higher (0".1–0".2) resolution can be critical in both distinguishing between morphologically normal and abnormal galaxies (e.g., BO 239) and revealing very close multiple systems. An excellent example of the latter is CN 22 in AC 114 whose double structure on the *HST* frames would have been missed at 0".45 resolution. However, the limiting surface brightness also plays an important role in morphological classifications and even with ~6 hr exposures, our WFC frames are considerably shallower than LPM's data. The surface brightness limit of *HST* is partially compromised by the spherical aberration, however, and we can remain optimistic for an improvement in this respect after the refurbishment mission.

4.5. *Morphology and Star Formation*

We are now in a position to examine the connections between the morphologies determined in §§ 4.1 and 4.2 and the star formation characteristics determined from spectroscopy and photometry discussed in §§ 3.1 and 3.2.

A cursory inspection of Tables 3 and 4 shows obvious trends. The most convincing features are the large number of

TABLE 5

COMPARISON OF MORPHOLOGIES WITH LAVERY ET AL. 1992

Galaxy Identification	This Paper			Lavery et al.	
	Morphology	Interaction/Merger	Comments	Disk	Comments
BO 39.....	?	Merg	Merger remnant, three tidal tails, tidal prominences	y	Interacting, separation 0".9, tidal tails
SMFC 12.....	D	Dist	Lies on arclet	y	Companion 2".5 NE?, tail or arclet
BO 128.....	D	Sat(2".2)	...	y	Interacting, small companion 2".2 SW
BO 165.....	D	Dist	...	y	Interacting, companion 3" NW
BO 181.....	E	...	...	y:	Isolated
BO 239.....	D(pec)	Merg?	Disturbed system	...	Isolated? galaxy 5" NE
BO 236.....	D	Sat(0".9, 1".2)	Triple system	...	Companion 1".4 N
BO 256.....	B	...	...	...	Isolated? galaxy 4" NW, tail?

TABLE 6

MORPHOLOGY STATISTICS

SPECTRAL CLASS	INTERACTION/MERGER			MORPHOLOGY				
	n_{obj}	$n_{I/M}$	$n_{I/M}/n_{obj}$ (%)	n_B[a]	n_I[b]	n_D[c]	n_U[d]	B/I/D (%)
AC 114								
E/S0	20	4	20	16	4	0	...	80/20/0
HDS	5	0	0	4	1	0	...	80/20/0
Starburst + PSG	5	3	60	1	2	2	...	20/40/40
Spiral	1	0	0	0	0	1	...	0/0/100
Abell 370								
E/S0	21	7	33	18	3	0	...	86/14/0
HDS	2	1:	50:	1	0	1	...	50/0/50
UVX	11	3	27	8	2	1	...	73/18/9
IRX	10	3	30	10	0	0	...	100/0/0
Blue	7	4	57	2	0	4	1	33/0/67
Overall								
E/S0	41	11	27	34	7	0	...	83/17/0
HDS	7	1:	14:	5	1	1	...	72/14/14
UVX + IRX	21	6	29	18	2	1	...	86/9/5
Blue	13	7	54	3	2	7	1	25/17/58

[a] Includes galaxies with Hubble typings cD/D, E, and S0.
[b] Includes galaxies with Hubble typings Sa–Sb.
[c] Includes galaxies with Hubble typings Sc–Sd.
[d] Number with uncertain morphology.

interacting/merging systems among the starburst and PSG galaxies and the close agreement between the morphological and spectroscopic typing for the red E/S0 population.

We quantify this further by presenting in Table 6 statistics on the incidence of interactions/mergers and morphologies for the different *spectroscopic* classes defined in § 3.1 for AC 114 (see Fig. 4) and Abell 370 and for the *photometric* classes of red objects in Abell 370 defined in § 3.2. We note that the spectroscopic groupings were used slightly differently for Abell 370 since the blue galaxy classifications are too insecure to define the starburst + PSG and spiral subgroupings as clearly as in AC 114. In presenting the morphological data we use the B, I, D bulge-disk scheme, with those galaxies for which a specific Hubble type was possible assigned as follows: E/S0 ≡ B, Sa–Sb ≡ I, and Sc–Sd ≡ D.

Examining the incidence of interactions/mergers first, a similar pattern is seen in both clusters with the highest rate, ~55%, seen among the blue galaxy population. Furthermore, if we exclude from consideration the Abell 370 members BO 236 and BO 239, whose spectroscopic classifications are either unknown or uncertain, then we find that all the interacting/merging systems among the blue members are spectroscopically classed as starburst or PSG galaxies (i.e., none have normal spiral galaxy spectra).

The dominant E/S0 population provides an important control sample in this respect. Here we find a lower (but nonnegligible) interaction/merger rate of 20% in AC 114 and 33% in Abell 370. And, importantly, the HDS sample has only one very marginal case of an interaction among the seven galaxies of this type in the two clusters. The rate is no higher in any of the photometrically peculiar E/S0s in Abell 370. Indeed, the vast majority of the UVX and IRX galaxies are bulge-dominated systems, and the fraction involved in mergers/interactions is also ≃30%.

If we take the red E/S0s as a control sample, the excess interaction/merger rate associated with the starburst + PSG population is not yet statistically significant. This is partially because the WFC field is sufficiently small that the current samples are lacking in blue members, most of which lie outside the core regions. Nonetheless, the interaction hypothesis must surely gain support from our verification of LPM's analysis and the individual cases of close mergers for the spectroscopic blue starbursts and PSG in three out of five cases in AC 114. In most cases, the interaction is between sources of comparable luminosities. Across both clusters only two to three out of the nine cases are in the "satellite" category defined in § 4.1.

Turning to the statistics on individual morphology, the most striking trend is the morphological distinction between the red and blue galaxy populations. The red members, irrespective of their E/S0, HDS, UVX, or IRX spectroscopic/photometric typing, show an ~85%:15% split between bulge-dominated and intermediate morphologies with an almost complete absence of the disk-dominated class. This profile in morphology over the B, I, D classes is very much representative of that seen in the cores of rich clusters at the present day (Dressler 1980a; Butcher & Oemler 1984).

In contrast, the blue members have a morphological distribution skewed toward the disk-dominated class: 58% of the blue galaxies within AC 114 and Abell 370 lie in this category. This consolidates the indications from previous ground-based studies (Thompson 1986; LPM) that the blue members of distant clusters are predominantly disk systems. With the caveat that clear spiral-arm structure has only been identified in one case here (No. 74 in AC 114), the disk-dominated nature of the blue objects is also consistent with DOBG's claim, based on *HST* imagery of a rich cluster at $z = 0.41$, that the blue populations in distant clusters are dominated by normal late Hubble types. Whereas a high fraction are involved in interactions/mergers, clearly the decline of this disk-dominated population is the heart of the BO effect.

Finally, identifying S0s at $z \simeq 0.35$ is a crucial aspect of testing the ram-pressure stripping hypothesis. Unfortunately, our difficulty in distinguishing between E and S0s (see § 4.2) precludes a detailed examination of this question. Nonetheless, some S0s are clearly seen (e.g., CN 159 in Fig. 6), and it is significant that none lie in the HDS category. Indeed, not one of the objects where we can be highly confident of its S0 classification, as a result of its high inclination or the presence of a distinctive disk, displays any indication of recent star formation.

5. DISCUSSION

We have clearly demonstrated that *HST* can provide valuable morphological data on distant cluster galaxies which, when combined with ground-based spectroscopic and multicolor information, offers a powerful and hitherto unavailable combination with which to confront the models proposed to explain the BO effect. As well as making broad statements about the morphology of cluster galaxies, we can focus on specific types of objects, particularly those which are the sites of ongoing or recent starburst activity. However, we recognize that with only two clusters, and a relatively small sample of blue members, our conclusions must be necessarily tentative pending the acquisition of further data. On the other hand we have a large sample of well-studied early-type galaxies including those characterized as HDS from high S/N spectroscopy in AC 114 and those with ultraviolet and infrared excesses in Abell 370.

There are four key observations to emerge from our study which most directly challenge the details of any model which proposes to explain cluster galaxy evolution:

1. Interactions and mergers between galaxies were a common occurrence in the cores of rich clusters at $z = 0.3$–0.4: in the two clusters studied here we see a 50%–60% occurrence among the blue galaxies and 20%–30% among the "dormant" red E/S0 population.
2. There appears to be good evidence that interactions/mergers provide a trigger of starburst activity. Those blue galaxies involved in a close interaction and/or merger are all spectroscopically classified as either starburst or PSG. However, there are a few starburst and PSG objects which appear isolated and show no morphological abnormalities.
3. Most of the blue galaxies are disk-dominated systems which are conspicuously absent in present-day clusters—a result confirmed independently by DOBG.
4. The anomalous early-type galaxies, namely the HDS, UVX, and IRX galaxies, interpreted as having recently ($\Delta\tau \simeq 1$–2 Gyr) completed a substantial burst of star formation in an otherwise dormant galaxy, show little or no evidence for any preferred involvement in interactions/mergers. Most are bulge-dominated systems, with a notable number being round ellipticals.

The high rate of interactions and mergers is unexpected if these galaxies are independent, dynamically well-mixed cluster members. While the density of galaxies in rich clusters is high, the large relative velocities between galaxies are thought to render interactions ineffective. The number of interacting and/or merging systems may therefore, as suggested by LPM, be telling us about the origin of these galaxies. If they represent a dynamical population with low relative velocity dispersion, they may originate in the surrounding field.

In the hierarchical picture for cluster growth, infall of systems with a range of scales is expected (Bower 1991). Galaxies in merging systems with low multiplicity have spent most of their lifetimes in regions with conditions similar to those in the field. Such newly acquired members should thus resemble field galaxies at $z \simeq 0.3$–0.4. It is therefore of much interest that faint-field galaxy surveys of this mean depth (Broadhurst, Ellis, & Shanks 1988; Colless et al. 1990, 1993a) reveal a strong increase in the mean star formation rate as measured with the equivalent width of the [O II] 3727 Å emission line (Ellis 1993). Moreover, high-resolution imaging of the field samples suggests that the strongest star-forming systems have multiple nuclei (Colless et al. 1993b), in striking similarity to the examples presented here. The high fraction of late-type galaxies in the blue population would also be naturally explained if these sources had recently arrived from the field.

Regardless of the origin of the interacting systems, it is clear that their enhanced star formation plays an important, if not dominant, role in producing the excess number of blue galaxies that originally attracted Butcher & Oemler's attention. We are, however, still left with the problem of the paucity of disk-dominated galaxies in present-day rich clusters. The nature of any present-day counterparts depends on the effects of merging and the subsequent star formation histories.

Although our sample of merging systems is still fairly small, we are struck by the comparable masses of the components involved which, according to numerical simulations, produce spheroidal systems fairly quickly (Barnes & Hernquist 1991). If the HDS systems are a later stage of the starburst phenomenon, as proposed by many investigators, the $\simeq 1$ Gyr timescale set by the continued presence of Balmer lines is considerably longer than the short ($\simeq 0.1$ Gyr) duration of the burst phase. One would therefore expect to see an order of magnitude more HDS and PSG examples than starburst systems. Unfortunately, without knowing the specific burst characteristics, the application of such a test is complicated by the bias toward starburst galaxies due to their increased optical luminosity during the star-forming phase. CS estimated this brightening could be as much as 2 mag in R. Additionally, the HST samples are currently concentrated to the inner regions, which may not yield representative fractions.

We must also take seriously the alternative viewpoint that the starburst and HDS phenomena are unrelated. Because HDS galaxies are extremely rare in the field population, their cause almost certainly lies in the cluster environment. An important clue in this respect is the recent study of early-type galaxies in the Coma cluster by Caldwell et al. (1993) in which $\sim 30\%$ of the population in a region about 1 Mpc from the core display the same HDS spectral signatures discussed in this work. Significantly, the spatial distribution of these "active" galaxies correlates well with a secondary peak in the X-ray emission found by Briel, Henry, & Böhringer (1992) which is interpreted as a gravitationally bound structure with its own intracluster medium and spheroidal members falling into Coma.

As we proceed to higher redshift, it is natural for such manifestations of hierarchical merging to become more frequent in the central regions of clusters. Indeed, preliminary evidence for this has been reported by Mushotsky (1993) on the basis of *ROSAT* imaging of a sample of distant BO clusters. Dynamical and gravitational lensing studies of Abell 370 (SMFC; Kneib et al. 1993) provides evidence for significant substructure associated with the cluster's two D galaxies. Kneib et al.'s well-constrained lensing model consists of two 800 km s^{-1}

masses centered on the D galaxies and is convincing evidence for the dynamical immaturity of this system. Such substructures complicate any simple analysis of the possible segregation between blue and red members.

In conclusion, we see from the discussion of our observations that a more coherent, albeit more complex, understanding of the BO effect and the underlying physical processes is emerging. It seems likely that no single process is wholly responsible for the effect; rather, a number of different processes govern the star formation activity within individual cluster galaxies. Further clarification will be possible when new high-resolution X-ray imagery of the distant clusters is combined with the *HST*-based morphologies and ground-based spectroscopy. Another important step to furthering our understanding will be to acquire morphological information for a larger sample of distant clusters. The expansion of our *HST* study to include further clusters within the CS sample will be reported in the next paper in this series.

We thank staff at the Space Telescope European Coordinating Facility, particularly Hans-Martin Adorf, Richard Hook, and Bob Fosbury for their expert assistance in processing our *HST* data. We are grateful to Alan Dressler, Gus Oemler, Jim Gunn, and Harvey Butcher for sharing their data on Abell 370 and in particular to Alan Dressler for preprocessing the images. Useful discussions with Richard Bower, Alan Dressler, Gus Oemler, Simon White, and Stephen Zepf are also gratefully acknowledged. W. J. C. acknowledges the financial support of the Australian Research Council, the Australian Academy of Science, and the Royal Society, and R. S. E. acknowledges financial support from the UK Science and Engineering Research Council.

REFERENCES

Adorf, H. M. 1993, in Science with *HST*, ed. P. Benvenuti & E. Schreier (Baltimore: STScI), 227
Allington-Smith, J. R., Ellis, R. S., Zirbel, E. L., & Oemler, A. 1993, ApJ, 404, 521
Aragón-Salamanca, A., Ellis, R. S., & Sharples, R. M. 1991, MNRAS, 248, 128
Barnes, J. E., & Hernquist, L. E. 1991, ApJ, 370, L65
Bower, R. G. 1991, MNRAS, 248, 332
Bower, R. G., Lucey, J. R., & Ellis, R. S. 1992, MNRAS, 254, 601
Briel, U. G., Henry, J. P., & Böhringer, H. 1992, A&A, 259, L31
Broadhurst, T. J., Ellis, R. S., & Shanks, T. 1988, MNRAS, 235, 827
Butcher, H., & Oemler, A. 1978, ApJ, 279, 18
———. 1984, ApJ, 285, 426
Butcher, H., Oemler, A., & Wells, D. C. 1983, ApJS, 52, 183
Caldwell, N., Rose, J. A., Sharples, R. M., & Ellis, R. S. 1993, AJ, 106, 508
Colless, M., Ellis, R. S., Broadhurst, T. J., Taylor, K., & Peterson, B. A. 1993a, MNRAS, 261, 19
Colless, M., Ellis, R. S., Taylor, K., & Hook, R. N. 1990, MNRAS, 244, 408
Colless, M., Schade, D. J., Broadhurst, T. J., & Ellis, R. S. 1993b, preprint
Couch, W. J., Ellis, R. S., Carter, D., & Godwin, J. 1983, MNRAS, 205, 1287
Couch, W. J., & Newell, E. B. 1984, ApJS, 56, 143
Couch, W. J., & Sharples, R. M. 1987, MNRAS, 229, 423 (CS)
Dressler, A. 1980a, ApJ, 236, 351
———. 1980b, ApJS, 42, 565
———. 1986, in Spectral Evolution of Galaxies, ed. C. Chiosi & A. Renzini (Dordrecht: Reidel), 375
———. 1993, in Observational Cosmology, ed. G. Chincarini, A. Iovino, T. Maccacaro, & D. Maccagni (San Francisco: ASP), 225
Dressler, A., & Gunn, J. E. 1982, ApJ, 263, 533
———. 1983, ApJ, 270, 7
———. 1990, in Evolution of the Universe of Galaxies, ed. R. G. Kron (San Francisco: ASP), 200
Dressler, A., Oemler, A., Butcher, H., & Gunn, J. E. 1994, ApJ, 430, 107 (DOBG)
Dressler, A., Oemler, A., Gunn, J. E., & Butcher, H. 1993, ApJ, 404, L45
Ellis, R. S. 1993, in Sky Surveys: Protostars to Protogalaxies, ed. T. Soifer 165
Ellis, R. S., Couch, W. J., MacLaren, I., & Koo, D. C. 1985, MNRAS, 217, 239
Elson, R. A. W., & Schade, D. J. 1993, in Science with *HST*, ed. P. Benvenuti & E. Schreier (Baltimore: STScI), 239
Evrard, G. 1991, MNRAS, 248, 8
Gunn, J. E., & Gott, J. R. 1972, ApJ, 176, 1
Guiderdoni, B., & Rocca-Volmerange, B. 1987, A&A, 186, 1
Henry, J. P., & Lavery, R. J. 1987, ApJ, 323, 473 (HL)
Kneib, J.-P., Mellier, Y., Fort, B., & Mathez, G. 1993, A&A, 273, 367
Krist, J. 1992, TINYTIM User's Manual (Baltimore: STScI)
Lawry, R. J., & Henry, J. P. 1986, ApJ, 304, L5
———. 1988, ApJ, 330, 596
Lavery, R. J., Pierce, M. J., & McClure, R. D. 1992, AJ, 104, 2067 (LPM)
Lucy, L. 1974, AJ, 79, 745
MacLaren, I., Ellis, R. S., & Couch, W. J. 1988, MNRAS, 230, 249
Mushotsky, R. 1993, in Ann. NY Acad. Sci. No. 688, Texas/PASCOS '92 Relativistic Astrophysics and Particle Cosmology, ed. C. W. Akerlof & M. A. Srednicki, 184
Oemler, A. 1992, in Clusters and Superclusters of Galaxies, ed. A. C. Fabian (Dordrecht: Kluwer), 29
Soucail, G., Mellier, Y., Fort, B., & Cailloux, M. 1988, A&AS, 73, 471 (SMFC)
Soucail, G., Mellier, Y., Fort, B., Picat, J. P., & Cailloux, M. 1987, A&A, 184, 361
Thompson, L. A. 1986, ApJ, 300, 639
Toomre, A., & Toomre, J. 1972, ApJ, 178, 623